Pathways for Neoarchean pyrite formation constrained by mass-independent sulfur isotopes

James Farquhar[a,b,1], John Cliff[b], Aubrey L. Zerkle[c], Alexey Kamyshny[d], Simon W. Poulton[e], Mark Claire[f], David Adams[b], and Brian Harms[a]

[a]Department of Geology and Earth System Science Interdisciplinary Center, University of Maryland, College Park, MD 20742; [b]Centre for Microscopy and Microanalysis, University of Western Australia, Perth, WA 6009, Australia; [c]School of Civil Engineering and Geosciences, Newcastle University, Newcastle upon Tyne NE1 7RU, United Kingdom; [d]Department of Geological and Environmental Sciences, Faculty of Natural Sciences, Ben-Gurion University of the Negev, Beer Sheva 84105, Israel; [e]School of Earth and Environment, University of Leeds, Leeds LS2 9JT, United Kingdom; and [f]School of Environmental Sciences, University of East Anglia, Norwich NR4 7TJ, United Kingdom

Edited by Mark H. Thiemens, University of California at San Diego, La Jolla, CA, and approved December 28, 2012 (received for review November 1, 2012)

It is generally thought that the sulfate reduction metabolism is ancient and would have been established well before the Neoarchean. It is puzzling, therefore, that the sulfur isotope record of the Neoarchean is characterized by a signal of atmospheric mass-independent chemistry rather than a strong overprint by sulfate reducers. Here, we present a study of the four sulfur isotopes obtained using secondary ion MS that seeks to reconcile a number of features seen in the Neoarchean sulfur isotope record. We suggest that Neoarchean ocean basins had two coexisting, significantly sized sulfur pools and that the pathways forming pyrite precursors played an important role in establishing how the isotopic characteristics of each of these pools was transferred to the sedimentary rock record. One of these pools is suggested to be a soluble (sulfate) pool, and the other pool (atmospherically derived elemental sulfur) is suggested to be largely insoluble and unreactive until it reacts with hydrogen sulfide. We suggest that the relative contributions of these pools to the formation of pyrite depend on both the accumulation of the insoluble pool and the rate of sulfide production in the pyrite-forming environments. We also suggest that the existence of a significant nonsulfate pool of reactive sulfur has masked isotopic evidence for the widespread activity of sulfate reducers in the rock record.

Neoarchean polysulfide production pathways | $\delta^{34}S$ | $\Delta^{33}S$ | $\Delta^{36}S$

Over the past 30 y, a significant amount of sulfur isotope data has been collected for sedimentary rocks and used as a way to study past atmospheric chemistry and biological activity. One feature of the sulfur isotope record that has been well-documented in the literature is a change from a relatively small range of variability for $\delta^{34}S$ in Archean sediments to a larger range in younger sediments. Interpretations of the $\delta^{34}S$ $[(^{34}S/^{32}S)_{sample}/(^{34}S/^{32}S)_{V\text{-}CDT} - 1]$ record have linked this pattern primarily to changes in the way that organisms metabolize sulfur. Experiments have shown that the magnitude of sulfur isotope fractionation diminishes as sulfate concentrations decrease (1). At low sulfate concentrations, sulfate reducers express only small fractionations, because the sulfate reduction metabolism operates as a nearly unidirectional chain of metabolic steps, and the isotope effects associated with each of the individual metabolic steps are not expressed in the final metabolic product (cf. 2). This microbial response to sulfate concentration has been invoked as the principle reason for the small range of $\delta^{34}S$ observed early in the geologic record, suggesting that sulfate concentrations were lower in Earth's early oceans. It is not known if other factors also played a part in generating the small range of $\delta^{34}S$ fractionations observed in the Neoarchean. We note that very large fractionations can occur at only slightly higher sulfate concentrations (1.1–2 mM) (3) and that the low concentration limit for generation of large fractionations associated with sulfate reduction may eventually be revised.

Another feature of the sulfur isotope record is revealed by the $\Delta^{33}S$ values of pyrite and sedimentary sulfate, which provide additional information about the evolution of the sulfur cycle. The range of variability for $\Delta^{33}S$ is significantly greater in samples older than ~2.4 Ga than in younger samples (e.g., compilation in refs. 4 and 5). This observation has been linked to the production, transfer, and preservation of mass-independent sulfur isotope signals (presumably of atmospheric origin) early in Earth history. The production of this signal in the atmosphere and its subsequent transfer to the Earth surface is sensitive to atmospheric O_2 levels and the redox state of sulfur in the atmosphere (6). Furthermore, the preservation of a mass-independent signal in the sedimentary record is sensitive to the intensity of redox cycling of sulfur in surface environments, which is greater in an oxidized world (4, 7, 8). The disappearance of the large range in $\Delta^{33}S$ variability from the geologic record at ~2.4 Ga has, therefore, been attributed to the rise of atmospheric oxygen. Studies that have looked at the late Archean sulfur cycle in detail have also argued that the mean value for the samples analyzed thus far shows a positive $\Delta^{33}S$ bias (9). The origin of this bias is not understood but may be linked to the identity of the sulfur pools in the early oceans and the transfer of sulfur from these pools to sedimentary pyrite in the late Archean.

In addition to $\delta^{34}S$ and $\Delta^{33}S$ records, $\Delta^{36}S$ records for the late Archean have also received a great deal of attention. The majority of $\Delta^{33}S$ vs. $\Delta^{36}S$ data presented for the late Archean converges on the origin ($\Delta^{33}S \sim \Delta^{36}S \sim 0$) and displays greater variability when $\Delta^{33}S$ and $\Delta^{36}S$ values are large. Some studies have noted (10, 11) that data from discrete stratigraphic intervals seem to define linear arrays with a constant slope ($\Delta^{36}S/\Delta^{33}S$). These arrays do not all intersect the origin but instead, often cross the axes at $\Delta^{33}S = 0$ and $\Delta^{36}S \neq 0$. Although the different relationships between $\Delta^{36}S$ and $\Delta^{33}S$ have been attributed to an atmospheric origin, it is unclear how important additional processes that are known to produce variations in $\Delta^{36}S$ (like sulfate reduction and pyrite formation) are for producing the observed compositional variability.

Here, we present results of secondary ion MS (SIMS) analyses (spot analyses) of sulfur isotope values in Neoarchean pyrites and explore these data with the specific goal of addressing some of the outstanding issues outlined above. This study has three aims. The first aim is to examine the origin and significance of the relationship between $\Delta^{36}S$ $[(^{36}S/^{32}S)_{sample}/(^{36}S/^{32}S)_{V\text{-}CDT} - [(^{34}S/^{32}S)_{sample}/(^{34}S/^{32}S)_{V\text{-}CDT}]^{1.9}]$ and $\Delta^{33}S$ $[(^{33}S/^{32}S)_{sample}/(^{33}S/^{32}S)_{V\text{-}CDT} - [(^{34}S/^{32}S)_{sample}/(^{34}S/^{32}S)_{V\text{-}CDT}]^{0.515}]$ in Neoarchean rocks. The second aim is to explore the nature of sulfur isotope evidence for sulfate reduction in Archean

Author contributions: J.F. and J.C. designed research; J.F., J.C., A.L.Z., A.K., S.W.P., M.C., D.A., and B.H. performed research; J.C. and D.A. contributed new reagents/analytic tools; J.F. and J.C. analyzed data; and J.F., J.C., A.L.Z., A.K., S.W.P., M.C., and B.H. wrote the paper.

The authors declare no conflict of interest.

This article is a PNAS Direct Submission.

[1]To whom correspondence should be addressed. E-mail: jfarquha@Glue.umd.edu.

This article contains supporting information online at www.pnas.org/lookup/suppl/doi:10.1073/pnas.1218851110/-/DCSupplemental.

environments, particularly whether the four isotopes of sulfur provide widespread evidence for sulfate reduction, even when the evidence provided by $\delta^{34}S$ alone is minor. The third aim is to explore the nature of the connections between different sulfur pools in the Archean sulfur cycle and to determine if there is evidence for an additional large standing sulfur pool in early oceanic and sedimentary environments. We examine whether these data are coherent at the grain scale, and what these data tell us about pathways for pyrite formation. We suggest that the generation of polysulfide in the Neoarchean may explain many poorly understood features of the sedimentary record of mass independent sulfur.

Samples

The samples investigated here are from the GKF01 drill core, which intersects well-preserved sediments of the ~2.65- to 2.5-Ga Campbellrand–Malmani carbonate platform (Ghaap Group, Transvaal Supergroup, South Africa) (12). Sample selection was guided by a previous study undertaken by Zerkle et al. (11). A subset of the strata studied by Zerkle et al. (11) was selected for more detailed analysis, with the aim of evaluating variations in the four sulfur isotopes at the grain and subgrain scale. Samples were also selected to test whether the nature of grain-scale isotopic heterogeneity measured by SIMS supports or contradicts hypotheses developed in the study by Zerkle et al. (11) on the basis of whole-rock SF_6 analyses.

Two types of samples were chosen for this study. One subset of samples consists of fine-grained laminated clastic lithologies (shales and siltstones) with small disseminated pyrites distributed along bedding planes. The pyrite grains range in size from a few microns to a few tens of microns. These samples permit evaluation of isotopic heterogeneity at the grain scale and between $\Delta^{33}S$ and $\Delta^{36}S$ for different pyrite grains. Another sample type (Fig. 1) is similar to that described by (13) and possesses a carbon-rich horizon with large ovoid pyrite grains of a few millimeters in their longest dimension and a few hundred microns in their shortest dimension. Overlaying the carbon-rich horizon is a fine- to medium-grained siltstone that hosts euhedral pyrite grains. In some cases, the euhedral grains overgrow the ovoid grains, and in other cases, the euhedral grains are isolated in the matrix. The euhedral pyrites range from 100 to 700 microns in their largest dimension.

Results

Results for analyses are presented in Figs. 2 and 3 as plots of $\delta^{34}S$ vs. $\Delta^{33}S$ and $\Delta^{33}S$ vs. $\Delta^{36}S$. These data illustrate a striking heterogeneity for $\delta^{34}S$ vs. $\Delta^{33}S$ in individual samples. However, they also reveal linear arrays in sulfur isotope values, mostly between $\Delta^{33}S$ and $\Delta^{36}S$ and sometimes, between $\delta^{34}S$ and $\Delta^{33}S$. These arrays are (*i*) distinct for different samples and (*ii*) intersect the composition for bulk $\Delta^{36}S$ and $\Delta^{33}S$ determined by analyses of bulk samples from approximately the same stratigraphic position (11).

There are differences in the $\delta^{34}S$ vs. $\Delta^{33}S$ arrays formed by pyrite grains between samples. For instance, the array formed in Fig. 2 for sample 829.5 (i.e., sampled from 829.5-m depth in the core) has a very steep slope on a plot of $\Delta^{33}S$ vs. $\delta^{34}S$, which is defined by an endmember with positive $\Delta^{33}S$ and $\delta^{34}S$ and another endmember with lower (possibly even negative) $\Delta^{33}S$ and positive $\delta^{34}S$. In contrast, the array formed for sample 1,102.6 is defined by one endmember with positive $\Delta^{33}S$ and $\delta^{34}S$ (similar to sample 829.5) and a second endmember with negative $\Delta^{33}S$ and significantly negative $\delta^{34}S$. Other samples yield data arrays intermediate between these two arrays (e.g., samples 1,404.6 and 888.3) or show clusters of data that fall within the broadly defined field of analyses made by SIMS and bulk chrome reduction techniques (samples 729.7 and 834.6). We note that sample 888.3 has what seems to be a texturally late vein cutting through an organic-rich part of this sample. This vein is ~20 microns across and discontinuous, with cross-cuts layering. The SIMS analyses yield a strongly negative $\delta^{34}S$, but the $\Delta^{33}S$ and $\Delta^{36}S$ are slightly mass-independent and follow the same relationship as disseminated grains in this sample. At least some of the sulfur in this vein is Archean in origin because

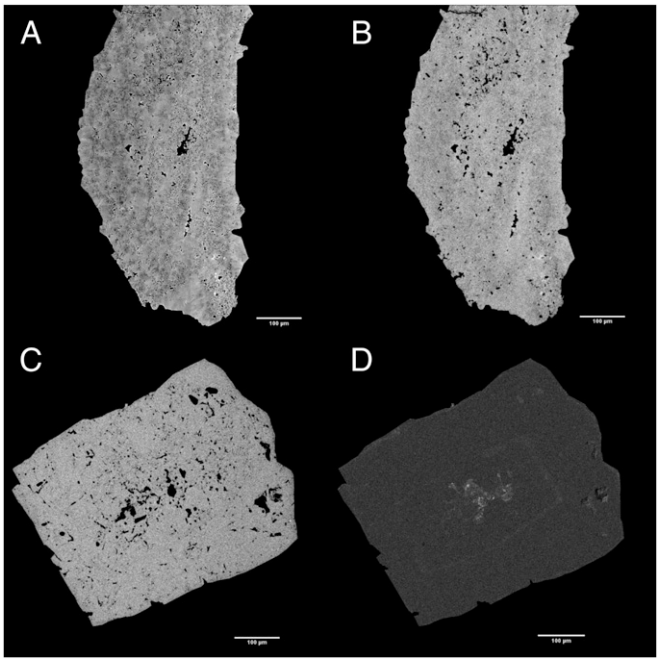

Fig. 1. Electron probe maps of ovoid (type 1) pyrite grains and euhedral (type 2) grains. (*A*) Backscatter secondary electron map of ovoid grain. (*B*) Fe map of ovoid grain. (*C*) Fe map of euhedral grain. (*D*) As map of euhedral grain.

of mass-independent fractionation (MIF), but the vein is also a texturally late feature, and it is not clear whether it formed shortly after the rock was consolidated or maybe tens or hundreds of millions of years after its formation. If the vein formed very late, it is possible that the strongly negative $\delta^{34}S$ reflects a late mass-dependent fractionation overprinted on mass-independent sulfur. Because of this uncertainty, we will not discuss this sample further, but work on this sample continues to understand its significance.

Sample 1,102.6, which contains two types of pyrite grains, yielded in situ analyses with both ^{34}S-depleted and -enriched compositions. It also preserved a relatively coherent relationship between $\Delta^{33}S$ and $\delta^{34}S$ and between $\Delta^{36}S$ and $\Delta^{33}S$ that seems to be broadly consistent with data from whole-rock analyses. Ovoid (type 1) pyrite grains are significantly ^{34}S-depleted relative to other rocks of this age, with negative $\delta^{34}S$ extending from −13‰ to −22‰. These grains have negative $\Delta^{33}S$ that is correlated with the $\delta^{34}S$ and ranges from values of approximately −0.4‰ to −1.0‰. These grains also have positive $\Delta^{36}S$ that ranges from values near zero to values slightly higher than 1‰. The euhedral (type 2) pyrite grains have positive $\delta^{34}S$ values, in contrast to the type 1 grains, which range from 5‰ to 22‰. The $\Delta^{33}S$ of the type 2 grains is also positive, ranging from about 5‰ to 10‰. These grains have negative $\Delta^{36}S$ values ranging from −12‰ to −4‰. The $\delta^{34}S$, $\Delta^{33}S$, and $\Delta^{36}S$ all seem to be correlated for the type 2 grains, and the arrays formed by multiple analyses of types 1 and 2 grains may be part of a single larger array (Figs. 1 and 2).

Discussion

Comparison of SF_6 and SIMS Measurements. In situ analyses of pyrite using SIMS have revealed striking heterogeneity for $\delta^{34}S$ and $\Delta^{33}S$ at the grain and subgrain scales (14, 15), which has raised questions about the interpretation of bulk rock centimeter-scale analyses undertaken by SF_6 methods. The SIMS analyses presented here also reveal heterogeneity for $\delta^{34}S$ and $\Delta^{33}S$ that was not resolved by the bulk chrome reduction preparation followed by SF_6 analyses presented by Zerkle et al. (11). Perhaps more importantly, the SIMS analyses presented here do not match the composition of all four sulfur isotopes presented in the study by

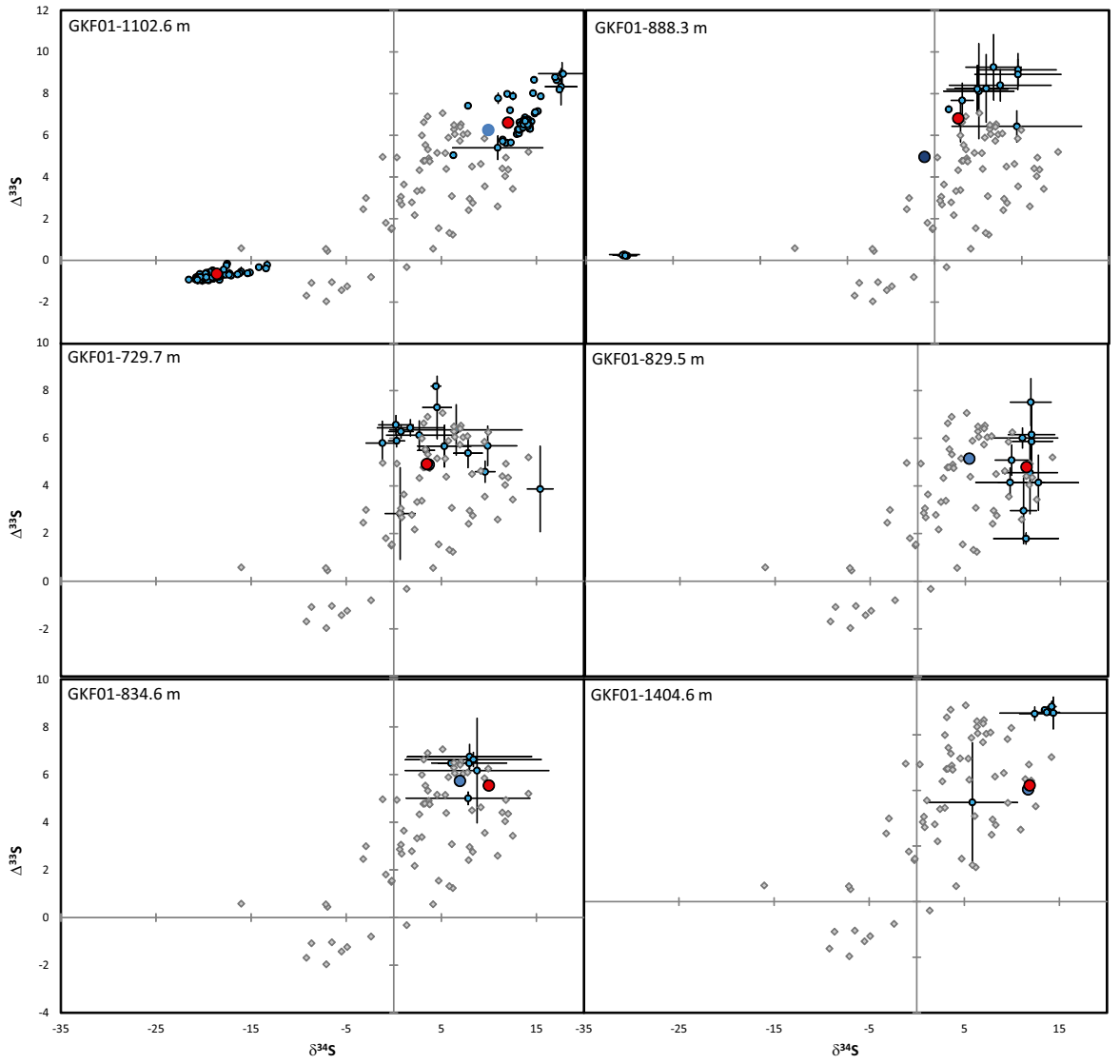

Fig. 2. Plot of $\Delta^{33}S$ vs. $\delta^{34}S$ illustrating SIMS analyses (small blue circles), bulk analyses of the same samples (larger red circles), bulk analyses of different splits of core at same depth in the work by Zerkle et al. (11) (large blue circle), and other analyses presented in the work by Zerkle et al. (11) (grey filled diamonds). The sample numbers refer to the depth from which they were sampled in the core. Error bars are estimates of 2σ. Lines on plots are simple regressions through SIMS data (constrained through origin for all but sample 1,102.6 m). Note that the samples from Zerkle et al. (11) for depths at 1,102.6 and 835.6 m were different from the samples analyzed here.

Zerkle et al. (11). In an effort to address this discrepancy, we have reanalyzed splits of the same samples and find that the agreement between SIMS methods and SF_6 analyses is better but still not perfect (data for samples at depths 888.3, 729.7, and 1,404.6 in Fig. 2). We are not certain whether the differences in $\Delta^{33}S$ and $\delta^{34}S$ between the SF_6 measurements and the mean values of the SIMS analyses are attributable to the fact that SIMS measurements were undertaken on closely related but technically different samples or whether the differences reflect real differences in grain size distribution or the sulfur species analyzed by the two techniques. Both techniques have limitations. SIMS analysis ensures that only pyrite is analyzed but requires grains that are larger than the primary ion beam, whereas chrome reduction techniques can extract all of the pyrite sulfur but also include sulfide phases other than pyrite (e.g., elemental sulfur and other sulfide phases).

The general field defined by all of the arrays for individual SIMS analyses overlaps with the field given by the SF_6 data but otherwise, shows no direct relationship with the whole-rock data. These differences presumably reflect differences in average signals as well as differences in the way that mass-independent signatures are overprinted by mass-dependent processes in Archean pyrite-forming environments.

We observe a consistent relationship between $\Delta^{36}S$ and $\Delta^{33}S$ values across larger stratigraphic intervals from grains measured for individual samples and whole-rock samples (Fig. 3). Variations in the relationship between $\Delta^{36}S$ and $\Delta^{33}S$ have been described in the studies in refs. 10, 11, 13, and 16–18 and are thought to reflect specific states of atmospheric sulfur chemistry. The existence of relatively stable arrays for $\Delta^{36}S$ vs. $\Delta^{33}S$ across stratigraphic intervals suggests linear mixing between two endmembers rather than mixing between three or more endmembers. Recently, Zerkle et al. (11) noted that stratigraphically resolved changes in the relationship between $\Delta^{36}S$ and $\Delta^{33}S$ for the GKF01 core also seem to be linked to coincident changes in $\delta^{13}C$ of organic carbon. Using atmospheric models, they suggested that shifts in the relationship between $\Delta^{33}S$ and $\Delta^{36}S$ arrays reflect a switch between atmospheric chemical states in response to a change in methane fluxes from the biosphere to the atmosphere. A feature of the linear

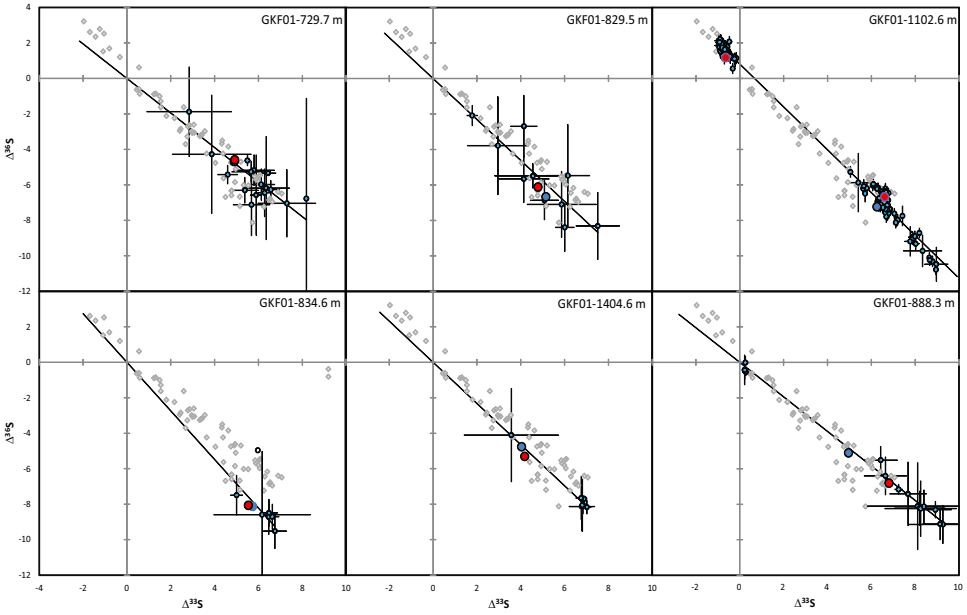

Fig. 3. Plots of $\Delta^{36}S$ vs. $\Delta^{33}S$ illustrating SIMS analyses (small blue circles), bulk analyses of the same samples (larger red circles), bulk analyses of different splits of core at same depth in the work by Zerkle et al. (11) (large blue circle), and other analyses presented in the work by Zerkle et al. (11) (grey filled diamonds). The sample numbers refer to the depth from which they were sampled in the core. Error bars are estimates of 2σ. Lines on plots are simple regressions through SIMS data (constrained through origin for all but sample 1,102.6 m).

mixing hypothesis is the inference that the arrays formed by individual grains within single samples will also be linear. SIMS measurements of different grains from the samples that we have analyzed form an array that includes the analyses by Zerkle et al. (11) and seem to support this assumption (Fig. 3). These data additionally suggest that measuring slopes in $\Delta^{36}S$ vs. $\Delta^{33}S$ using either SIMS or bulk extraction techniques could provide a useful geochemical tool in correlating different sections deposited around this time.

Evidence for Large S Isotope Fractionations by Sulfate Reducers. We interpret the negative $\delta^{34}S$ of the type 1 grains (sample 1102.6) to reflect sulfide production by sulfate reducers that were growing in an environment, where sulfate concentrations were sufficiently high to produce large sulfur isotope fractionations and the sulfate pool was sufficiently large that its composition was not significantly shifted as a result of complete consumption during sulfate reduction. If the sulfate was consumed entirely, one would not expect to see a relatively stable, strongly negative $\delta^{34}S$ in the product pyrite, even if the fractionations were large. This result suggests a relatively large pool of available sulfate at the time that the type 1 grains were formed and could imply that these grains formed in a setting that facilitated communication with the oceanic sulfate pool, such as at the sediment–water interface, implying sulfate exchange within the water column (eddy mixing rates) that were sufficient to outcompete sulfate drawdown by sulfate reducers (sulfate reduction rates). There are several implications of this interpretation. Three requirements explain our data.

i) The evidence for large fractionations in our samples may imply that sulfate concentrations were slightly above the concentration threshold suggested in ref. 1 or that this threshold should be revised to lower sulfate concentrations.

ii) The lack of evidence for large fractionations elsewhere in the Archean record implies either global sulfate concentrations below this threshold or that there is some other control on the expression of these large fractionations in pyrite—possibly associated with access to a sulfate pool that is not subject to draw down and Rayleigh fractionation.

iii) If it is the latter, sulfate concentrations were high enough in the sulfate pool to limit effects of drawdown and Rayleigh fractionation during precipitation of ovoid grains.

It also might be argued that evidence presented here is from a single sample and that sulfate concentrations were locally enhanced or unusually high at the time that the sample was deposited. We find it difficult to make a strong argument for this alternative, because it would require a mechanism for concentrating sulfate with negative $\Delta^{33}S$ in a system where most sulfur seems to have positive $\Delta^{33}S$. If there was a (local) basinal enhancement of sulfate concentrations, it would require a mechanism to raise sulfate concentrations. Salinity measurements in today's oceans and enclosed equatorial basins, where evaporation concentrates sulfate, such as the Mediterranean Sea, show enhancements of less than 20% relative to the open ocean (19). Although it is possible that evaporation in Archean basins may have concentrated sulfate to a greater degree than today, we do not favor this explanation for the observed large fractionations. We argue, instead, that sulfate concentrations may have been high enough in much of the Neoarchean to allow expression of large metabolic fractionations but that a combination of near-quantitative sulfate reduction and a second source of sulfide prevented the signatures of sulfate reduction from being preserved, implying that sulfate concentrations were high enough to allow for large fractionations to be expressed.

Experimental and field studies have suggested that large framboidal pyrite grains typically form in sulfide-rich environments and associated with rapid rates of pyrite formation, whereas euhedral pyrite grains form in settings where sulfide concentrations are lower and pyrite formation rates are slower (20–22). We interpret the type I (ovoid) pyrite grains as relict framboids, suggesting that the isotopic composition of these grains formed in a setting where sulfide was abundant and derived principally from an oceanic sulfate pool with negative $\Delta^{33}S$.

Evidence for pyrites with negative $\delta^{34}S$ and negative $\Delta^{33}S$ is rare in other Neoarchean successions, but it is not entirely absent. Pyrite from carbonates of the Wittenoom Fm. has been shown by Golding et al. (23) to have a similar signal. The scarcity of clear $\delta^{34}S$ and $\Delta^{33}S$ signals of sulfate reduction in the Neoarchean record might reflect (in part) the nature of the sulfur pools in Neoarchean depositional environments and the way that the sulfur isotope signatures from different sulfur pools were transferred to sedimentary pyrite precursors. We explore these possibilities next.

Nature of Sulfur Pools in the Neoarchean Oceans and Sediments. The clustering of sulfur isotope data into two fields defined by grain type in sample 1,102.6 suggests the presence of two sulfur pools in the environments in which these pyrites formed. One pool had strongly negative $\delta^{34}S$, negative $\Delta^{33}S$, and positive $\Delta^{36}S$, and another pool had strongly positive $\delta^{34}S$, positive $\Delta^{33}S$, and negative $\Delta^{36}S$. We are

suggesting that these pools are virtually contemporaneous and distinct and that the differences in isotopic composition do not reflect temporal evolution of a single pool.

Evidence from barite, volcanogenic massive sulfide deposits (VMS), komatiites, and carbonates (9, 24, 25) suggests that the negative $\Delta^{33}S$ pool in the Archean resided as oceanic sulfate, suggesting that the sulfur isotope record of Archean pyrite (which has positive $\Delta^{33}S$ mean and median values) is controlled by factors other than direct formation from the products of sulfate reduction.

The high proportion of Neoarchean pyrite measurements yielding positive $\Delta^{33}S$ suggests a significant contribution from a sulfur pool with positive $\Delta^{33}S$. The source of the positive $\Delta^{33}S$ and $\delta^{34}S$ sulfur in Neoarchean sediments has been a topic of considerable discussion (7, 13, 26, 27). We suggest that the preponderance of data with positive $\Delta^{33}S$ implies a standing sulfur pool in addition to the oceanic sulfate pool. We suggest that this standing pool derives from atmospheric deposition of zero valent sulfur that accumulated as insoluble compounds in Neoarchean sediments but that the distribution of this sulfur may not have been uniform across the globe. Zero valent sulfur species may have accumulated preferentially in sedimentary basins proximal to volcanic and biogenic sources of atmospheric sulfur gases because of atmospheric residence times on the order of days to weeks (6, 28).

Hypothesis Linking Sulfur Pools, Formation of Pyrite Precursors, and MIF S Records. We suggest that the pathways associated with the transfer of sulfur to pyrite can provide a way to reconcile a number of diverse aspects of the Archean sulfur isotope record. These pathways include (*i*) the bias to positive $\Delta^{33}S$ in the larger Neoarchean dataset (9), (*ii*) the preservation of pyrite with both positive and negative $\Delta^{33}S$, and (*iii*) the consistent $\delta^{34}S/\Delta^{33}S$ and $\Delta^{36}S/\Delta^{33}S$ arrays for analyses of both bulk sulfide and disseminated grains.

As discussed above, the appearance of two distinct populations of pyrite in Neoarchean samples like sample GKF01 1,102.6 could imply that pyrite sulfur was derived from two separate sulfur pools. ^{33}S-enriched pyrite presumably acquires most, if not all, of its sulfur from a pool with positive $\Delta^{33}S$, such as an atmospheric elemental sulfur pool (6, 28). In contrast, pyrite with strongly negative $\delta^{34}S$ and $\Delta^{33}S$ is inferred to be formed from sulfide produced by bacterial sulfate reduction of oceanic sulfate (or sulfite, if present) with negative $\Delta^{33}S$.

Luther (29) and Schoonen and Barnes (30) have suggested that one pathway for pyrite formation involves reaction between polysulfide and an iron sulfide. This pathway involves the transfer of at least one sulfur atom from polysulfide ions to form pyrite. Pyrite with positive $\Delta^{33}S$ could have acquired most of its sulfur from polysulfides that were produced when small amounts of biogenic sulfide reacted with atmospherically derived elemental sulfur. In this case, the relative proportion of sulfate-derived sulfur to sulfur derived from zero valent species would be small, and the zero valent species would control the isotopic composition. In contrast, pyrite exhibiting negative $\Delta^{33}S$ would have acquired its sulfur either directly from sulfide produced by sulfate reduction or from a polysulfide pool that had exchanged extensively with biologically produced sulfide, implying a mass balance that favored sulfate-derived sulfide over polysulfide-derived sulfide from a zero valent species.

We suggest that, for the different pyrites in sample 1,102.6, the ovoid (type 1) pyrites formed in a setting where sulfate-derived sulfide was abundant, and the euhedral (type 2) pyrites formed at a slightly later time in a setting with less sulfate-derived sulfide, where sulfur for pyrite formation was provided by polysulfide derived from an elemental sulfur precursor. An unresolved issue with this hypothesis is how the different forms of sulfur (sulfate-derived sulfide and zero valent-derived polysulfide) were supplied to the microenvironments where pyrite formation occurred. The sulfate pool would presumably have been present in soluble forms in the Neoarchean ocean, but the location of the elemental sulfur pool is less certain. This pool may have accumulated as an insoluble component of sediments that was later converted to a soluble, reactive, and mobile form of polysulfide when it reacted with small amounts of hydrogen sulfide produced by sulfate reducers.

Synthesis and Possible Implications. The hypotheses and data presented here can be synthesized as follows.

The relationship between $\Delta^{36}S$ and $\Delta^{33}S$ observed in the SIMS analyses is consistent with observations of this relationship in centimeter-scale samples measured using the SF_6 technique and reported in the work by Zerkle et al. (11). This compositional measure was interpreted as an atmospheric signature that reflected short-lived changes in atmospheric chemistry. Our observations here continue to support this hypothesis.

We suggest that Archean pyrite with positive $\Delta^{33}S$ (and possibly, the majority of Neoarchean pyrite) acquires its $\Delta^{33}S$ and $\Delta^{36}S$ from a standing pool of zero valent sulfur that is activated by reaction with H_2S. Formation of pyrite always requires the presence of sulfide; however, the $\Delta^{33}S$ signature preserved in this pyrite depends on the concentration of sulfide in the environment. In cases where sulfate reduction rates were low and sulfide production rates were low, the sulfur transferred to pyrite came from polysulfide ions that were formed as a result of reaction between small amounts of sulfide and larger amounts of atmospherically derived elemental sulfur with positive $\Delta^{33}S$. The ratio of sulfate-derived sulfur to zero valent sulfur at equilibrium with a soluble polysulfide pool is 3.6 at pH 8 and may be as high as 4.0 at pH 9 (31). Once formed, polysulfide and sulfide will exchange isotopes, but with a significant proportion of sulfur coming from elemental sulfur, the signature of sulfate will not be expressed except in cases where sulfate reduction rates are very high. In cases where sulfate reduction rates were high and sulfide concentrations were high, the sulfur transferred to pyrite came from polysulfides that were either derived from or have exchanged extensively with biologically produced sulfide with negative $\Delta^{33}S$.

This hypothesis can also partially explain why the majority of $\Delta^{33}S$ analyses of sulfur from the shales studied to date has shown a bias to positive values. These shales may come from marginal basins, where an atmospheric zero valent species preferentially accumulated and dominated the sulfur isotope signature of pyrite. This hypothesis would require relatively small contributions from sulfate-derived sulfide and may imply that atmospheric deposition of zero valent sulfur was concentrated in certain regions. We envision depositional basins that were proximal to biogenic (or volcanic) sources of atmospheric gases, such as H_2S, methylated sulfur gases (e.g., dimethyl sulfide or methane thiol), and possibly, sulfur dioxide. We suggest that heterogeneity in atmospheric deposition may reflect relatively rapid atmospheric production and subsequent short residence times for rainout of S_8 aerosols. On a global scale, sulfate sinks from the oceanic pool may have been associated with hydrothermal activity (e.g., VMS and Ni sulfide komatiite-hosted ores) (9, 24, 27) and possibly, sulfate reduction in systems, where less atmospherically derived zero valent sulfur was delivered.

This hypothesis could also reveal an important difference in the source of polysulfide before the rise of oxygen. Our isotopic data point to an anoxic world, where the pathways for production of polysulfides would have involved reaction between hydrogen sulfide and an atmospherically derived elemental sulfur species. After the rise of oxygen (such as in modern environments), polysulfides would, instead, derive principally from oxidation of biogenically produced sulfide by Mn^{4+}, Fe^{3+}, or oxygen (31–34).

Finally, this hypothesis may also provide a way to understand the paucity of isotopic evidence for bacterial sulfate reduction in the Neoarchean—a time when other evidence suggests that these organisms were active. The changes in $\Delta^{33}S$ and $\Delta^{36}S$ that we observe for different pyrite grains could be explained by mixing of sulfide sulfur produced by sulfate-reducing bacteria with sulfur derived from a zero valent pool. The lack of evidence for strongly negative $\delta^{34}S$ for much of the Archean pyrite analyzed to date could reflect a predominant source for pyrite sulfur other than biologically produced sulfide (e.g., polysulfides).

The data presented here provide evidence for $\delta^{34}S$ fractionations in pyrite approaching 30‰ in one Neoarchean setting. This estimate is obtained by assuming that Neoarchean seawater had a $\delta^{34}S$ value of ~10‰ (9, 27). The magnitude of this fractionation is large, and it is not clear how fractionations of this magnitude can be

reconciled with the present consensus that sulfate concentrations in the Archean oceans were below a threshold for expression of large fractionations between sulfate and buried pyrite (1). Note that some arrays seen on plots of $\delta^{34}S$ vs. $\Delta^{33}S$ also suggest an end-member with strongly negative $\delta^{34}S$ (14).

If the strongly negative $\delta^{34}S$ observed here for grains from the sample at 1,102.6 m reflects sulfate reduction at the sediment–water interface, it may indicate that sulfate concentrations in ocean water were above the threshold for bacteria to produce large fractionations but that, when pyrite formation occurred within sediments, drawdown of sulfate in the sediments, combined with the added contributions of sulfur ultimately derived from zero valent sulfur, prevented a clear signal of large sulfur isotope fractionations from being preserved. One thing that we find striking is the rarity of evidence for strongly negative $\delta^{34}S$ and negative $\Delta^{33}S$ signatures of sulfate reduction in organic-rich Neoarchean shales, which suggests that most of the sulfur in these pyrites and also, pyrite analyzed from other Neoarchean successions comes from a nonsulfate–sulfur pool. This bias may, in part, reflect masking of signals caused by bulk analysis techniques, but we suggest here that it also reflects a broader process related to pyrite formation.

Materials and Methods

Sulfur four-isotope ratios ($^{x}S/^{32}S$) were determined using a Cameca IMS 1280 ion microprobe in multicollection mode. In all cases, NMR regulation was used, and ^{32}S, ^{33}S, and ^{34}S were measured using Faraday cup detectors. ^{36}S was measured using an electron multiplier. Details of the methods are described in *SI Appendix*. SF_6 analyses were undertaken using standard fluorination techniques and isotope ratio MS using a Thermo Finnigan MAT 253 at the University of Maryland. Preparation of silver sulfide (used for fluorination) and SF_6 as well as the MS are described in ref. 11. X-ray maps were obtained using a JEOL 8530F microprobe, using a 20-kV, 100-nA point beam and a pixel dwell time of 85 ms.

ACKNOWLEDGMENTS. The authors thank Sten Littmann, Marco Fiorentini, and Boz Wing for help in development of ion probe sulfide standards and also thank reviewers who provided comments that improved the clarity of the manuscript. The authors acknowledge the facilities and the scientific and technical assistance of the Australian Microscopy and Microanalysis Research Facility at the Centre for Microscopy, Characterisation and Analysis, University of Western Australia, a facility funded by the University, State, and Commonwealth Governments. We acknowledge support from the National Aeronautics and Space Administration (NASA) exobiology program, the NASA Astobiology Institute, the Natural Environment Research Council, and the University of Western Australia for the award to J.F. of the Gledden Senior Fellowship.

1. Habicht KS, Gade M, Thamdrup B, Berg P, Canfield DE (2002) Calibration of sulfate levels in the archean ocean. *Science* 298(5602):2372–2374.
2. Hayes JM (2001) Fractionation of carbon and hydrogen isotopes in biosynthetic processes. *Rev Mineral Geochem* 43:225–277.
3. Canfield DE, Zerkle AL, Farquhar J (2010) High isotope fractionations during sulfate reduction in a low-sulfate euxinic ocean analog. *Geology* 38:415–418.
4. Farquhar J, Zerkle AL, Bekker A (2011) Geological constraints on the origin of oxygenic photosynthesis. *Photosynth Res* 107(1):11–36.
5. Halevy I, Johnston DT, Schrag DP (2010) Explaining the structure of the Archean mass-independent sulfur isotope record. *Science* 329(5988):204–207.
6. Pavlov AA, Kasting JF (2002) Mass-independent fractionation of sulfur isotopes in Archean sediments: Strong evidence for an anoxic Archean atmosphere. *Astrobiology* 2(1):27–41.
7. Farquhar J, Bao HM, Thiemens M (2000) Atmospheric influence of Earth's earliest sulfur cycle. *Science* 289(5480):756–759.
8. Stüeken EE, Catling DC, Buick R (2012) Contributions to late Archaean sulphur cycling by life on land. *Nat Geosci* 5:722–725.
9. Farquhar J, Wing BA (2005) The terrestrial record of stable sulphur isotopes: A review of the implications for evolution of Earth's sulphur cycle. *Mineral Deposits and Earth Evolution*, eds Mcdonald I, Boyce AJ, Butler IB, Herrington RJ, Polya DA (Geological Society, London, Special Publications, London), Vol 248, pp 167–177.
10. Kaufman AJ, et al. (2007) Late Archean biospheric oxygenation and atmospheric evolution. *Science* 317(5846):1900–1903.
11. Zerkle AL, Claire M, Domagal-Goldman SD, Farquhar J, Poulton SW (2012) A bistable organic-rich atmosphere on the Neoarchaean Earth. *Nat Geosci* 5(5):359–363.
12. Schroder S, Lacassie JP, Beukes NJ (2006) Stratigraphic and geochemical framework of the Agouron drill cores, Transvaal Supergroup (Neoarchean-Paleoproterozoic, South Africa). *S Afr J Geol* 109(1–2):23–54.
13. Ono SH, Beukes NJ, Rumble D (2009) Origin of two distinct multiple-sulfur isotope compositions of pyrite in the 2.5 Ga Klein Naute Formation, Griqualand West Basin, South Africa. *Precambrian Res* 169(1–4):48–57.
14. Kamber BS, Whitehouse MJ (2007) Micro-scale sulphur isotope evidence for sulphur cycling in the late Archean shallow ocean. *Geobiology* 5(1):5–17.
15. Williford KH, Van Kranendonk MJ, Ushikubo T, Kozdon R, Valley JW (2012) Constraining atmospheric oxygen and seawater sulfate concentrations during Paleoproterozoic glaciation: In situ sulfur three-isotope microanalysis of pyrite from the Turee Creek Group, Western Australia. *Geochim Cosmochim Acta* 75(19):5686–5705.
16. Farquhar J, et al. (2007) Isotopic evidence for Mesoarchaean anoxia and changing atmospheric sulphur chemistry. *Nature* 449(7163):706–709.
17. Ono S, Beukes NJ, Rumble D, Fogel ML (2006) Early evolution of atmospheric oxygen from multiple-sulfur and carbon isotope records of the 2.9 Ga Mozaan Group of the Pongola Supergroup, Southern Africa. *S Afr J Geol* 109(1–2):97–108.
18. Domagal-Goldman SD, Kasting JF, Johnston DT, Farquhar J (2008) Organic haze, glaciations and multiple sulfur isotopes in the Mid-Archean Era. *Earth Planet Sci Lett* 269(1–2):29–40.
19. Antonov JI, Locarnini RA, Boyer TP, Mishonov AV, Garcia HE (2006) World ocean atlas 2005. *NOAA Atlas NESDIS 62*, ed Levitus S (US Government Printing Office, Washington, DC), Vol 2.
20. Sweeney RE, Kaplan IR (1973) Pyrite framboid formation—laboratory synthesis and marine sediments. *Econ Geol* 68(5):618–634.
21. Wilkin RT, Barnes HL, Brantley SL (1996) The size distribution of framboidal pyrite in modern sediments: An indicator of redox conditions. *Geochim Cosmochim Acta* 60 (20):3897–3912.
22. Passier HF, Middelburg JJ, de Lange GJ, Bottcher ME (1999) Modes of sapropel formation in the eastern Mediterranean: Some constraints based on pyrite properties. *Mar Geol* 153(1–4):199–219.
23. Golding SD, et al. (2011) Earliest seafloor hydrothermal systems on earth: Comparison with modern analogues. *Earliest Life on Earth: Habitats, Environments and Methods of Detection*, eds Golding SD, Glikson M (Springer Science+Business Media B.V., Berlin), pp 15–49.
24. Bekker A, et al. (2009) Atmospheric sulfur in Archean komatiite-hosted nickel deposits. *Science* 326(5956):1086–1089.
25. Fiorentini ML, et al. (2012) Multiple sulfur and iron isotope composition of magmatic Ni-Cu-(PGE) sulfide mineralization from eastern Botswana. *Econ Geol* 107(1):105–116.
26. Farquhar J, Wing BA (2003) Multiple sulfur isotopes and the evolution of the atmosphere. *Earth Planet Sci Lett* 213(1–2):1–13.
27. Ono S, et al. (2003) New insights into Archean sulfur cycle from mass-independent sulfur isotope records from the Hamersley Basin, Australia. *Earth Planet Sci Lett* 213(1–2):15–30.
28. Farquhar J, Savarino J, Airieau S, Thiemens MH (2001) Observation of wavelength-sensitive mass-independent sulfur isotope effects during SO_2 photolysis: Implications for the early atmosphere. *J Geophys Res Planets* 106(E12):32829–32839.
29. Luther GW (1991) Pyrite synthesis via polysulfide compounds. *Geochim Cosmochim Acta* 55(10):2839–2849.
30. Schoonen MAA, Barnes HL (1991) Reactions forming pyrite and marcasite from solution. 1. Nucleation of Fes2 below 100-degrees-C. *Geochim Cosmochim Acta* 55(6): 1495–1504.
31. Kamyshny A, Jr., Gun J, Rizkov D, Voitsekovski T, Lev O (2007) Equilibrium distribution of polysulfide ions in aqueous solutions at different temperatures by rapid single phase derivatization. *Environ Sci Technol* 41(7):2395–2400.
32. Yao WS, Millero FJ (1996) Oxidation of hydrogen sulfide by hydrous Fe(III) oxides in seawater. *Mar Chem* 52(1):1–16.
33. Yao WS, Millero FJ (1993) The rate of sulfide oxidation by delta-Mno2 in seawater. *Geochim Cosmochim Acta* 57(14):3359–3365.
34. Hoffmann MR (1977) Kinetics and mechanism of oxidation of hydrogen-sulfide by hydrogen-peroxide in acidic solution. *Environ Sci Technol* 11(1):61–66.